Acta Crystallographica Section F
Structural Biology and Crystallization Communications
ISSN 1744-3091

Expression, purification, crystallization and preliminary X-ray crystallographic analysis of Enpp1

Kazuki Kato,[a] Hiroshi Nishimasu,[a] Emiko Mihara,[b] Ryuichiro Ishitani,[a] Junichi Takagi,[b] Junken Aoki[c] and Osamu Nureki[a]*

[a]Department of Biophysics and Biochemistry, Graduate School of Science, The University of Tokyo, 7-3-1 Hongo, Bunkyo-ku, Tokyo 113-0033, Japan, [b]Institute for Protein Research, Osaka University, 3-2 Yamadaoka, Suita, Osaka 565-0871, Japan, and [c]Graduate School of Pharmaceutical Sciences, Tohoku University, 6-3 Aoba, Aramaki, Aoba-ku, Sendai, Miyagi 980-8578, Japan

Correspondence e-mail: nureki@biochem.s.u-tokyo.ac.jp

Received 4 April 2012
Accepted 30 April 2012

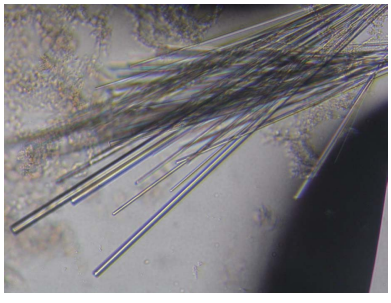

Enpp1 is an extracellular membrane-bound glycoprotein that regulates bone mineralization by hydrolyzing ATP to generate pyrophosphate. The extracellular region of mouse Enpp1 was expressed in HEK293S GnT1$^-$ cells, purified using the TARGET tag/P20.1-Sepharose system and crystallized. An X-ray diffraction data set was collected to 3.0 Å resolution. The crystal belonged to space group $P3_1$, with unit-cell parameters $a = b = 105.3$, $c = 173.7$ Å. A single-wavelength anomalous dispersion (SAD) data set was also collected to 2.7 Å resolution using a selenomethionine-labelled crystal. The experimental phases determined by the SAD method produced an interpretable electron-density map.

1. Introduction

Enpp1 (also known as PC-1) is an extracellular glycoprotein that hydrolyzes ATP to generate AMP and pyrophosphate (PP_i). PP_i inhibits the incorporation of inorganic phosphate into hydroxyapatite crystals and acts as a physiological inhibitor of bone and soft-tissue mineralization (Hessle *et al.*, 2002). Thus, Enpp1 negatively regulates bone mineralization and ectopic calcification. Loss-of-function mutations of Enpp1 are associated with the human disease GACI (generalized arterial calcification of infancy), which is characterized by ectopic calcification owing to low levels of extracellular PP_i (Rutsch *et al.*, 2003). However, the molecular mechanism by which these mutations impair the enzymatic activity remains unknown.

Enpp1 is the first member of the Enpp (ectonucleotide phosphodiesterase/pyrophosphatase) family, which consists of extracellular enzymes that are conserved in vertebrates from fish to mammals (Stefan *et al.*, 2005). The mammalian Enpp family comprises seven members (Enpp1–Enpp7). Enpp2 (also known as autotaxin) is a secreted protein, whereas the other Enpp-family members are membrane-spanning or glycosylphosphatidylinositol-anchored proteins. Enpp1–Enpp3 are multidomain proteins and consist of two somatomedin B (SMB)-like domains, a catalytic domain and a nuclease-like domain, whereas Enpp4–Enpp7 have only a catalytic domain and lack the SMB-like and nuclease-like domains. Although they share a similar catalytic domain belonging to the alkaline phosphatase superfamily, the Enpp-family members have different physiological functions depending on their distinct substrate specificity. Among the family members, Enpp2 hydrolyzes lysophosphatidylcholine to generate lysophosphatidic acid, a lipid mediator that activates G protein-coupled receptors. The recently reported crystal structures of Enpp2 from mouse (Nishimasu *et al.*, 2011) and rat (Hausmann *et al.*, 2011) revealed that lipid substrates are accommodated in the hydrophobic pocket in the catalytic domain. A sequence comparison between the Enpp members suggested that the insertion sequence in the catalytic domain is a major determinant of the substrate specificity of the members of the family (Nishimasu *et al.*, 2012).

2. Materials and methods

2.1. Construction

We constructed an expression plasmid encoding the extracellular region (residues 92–905) of mouse Enpp1 fused with the secretory

signal sequence (residues 1–50) and the N-terminal nine residues of the SMB1 domain (residues 51–59) of mouse Enpp2 at the N-terminus and the TARGET tag at the C-terminus. The TARGET tag consists of 21 amino acids (YPGQ×5 + V) and is specifically recognized by the P20.1 antibody (Tabata *et al.*, 2010). DNA fragments encoding full-length Enpp1 and Enpp2 from mouse were amplified by PCR using pCAG-GS-Enpp1 and pCAG-GS-Enpp2 as templates and PrimeSTAR MAX DNA polymerase (Takara Bio Inc.). The PCR products were inserted into the *Xba*I and *Kpn*I sites of pcDNA3.1 (Invitrogen), which had been modified to contain a C-terminal tobacco etch virus (TEV) protease cleavage site followed by the TARGET tag (referred to as pcD-CW; Tabata *et al.*, 2010). Nucleotides 271–279 of the Enpp1 gene (5′-AAAGGCCGC-3′) and nucleotides 175–183 of the Enpp2 gene (5′-AAAGGTAGA-3′) were replaced by the *Not*I site-containing sequence (5′-C**GCGGCCGC**-3′; the *Not*I site is shown in bold) using a PCR-based method. These nucleotides encode the N-terminal regions of the SMB1 domains of Enpp1 and Enpp2; Lys91 in the SMB1 domain of Enpp1 was replaced by Arg owing to the introduction of the *Not*I restriction site. pcD-CW-Enpp1 was digested with *Hin*dIII and *Not*I to prepare the pcD-CW vector containing the extracellular region of Enpp1. pcD-CW-Enpp2 was digested with *Hin*dIII and *Not*I to prepare the DNA fragment encoding the N-terminal secretory signal sequence and the N-terminal nine residues of the SMB1 domain of Enpp2. These DNA fragments were ligated to prepare the expression vector and the sequences were verified by DNA sequencing.

2.2. Expression

HEK293S GnT1$^-$ cells were cultured at 310 K in a humidified atmosphere containing 5% CO_2 using DMEM medium (Sigma) supplemented with 10%(*v*/*v*) FBS (Euro Clone), 1%(*v*/*v*) MEM non-essential amino acids (Sigma) and 1%(*v*/*v*) sodium pyruvate (Gibco). HEK293S GnT1$^-$ cells were transfected with the expression plasmid using the Lipofectamine 2000 reagent (Invitrogen). Stably transfected cell lines were screened using medium containing 1 mg ml^{-1} G418 (Nacalai Tesque) and were cloned by limiting-dilution analysis in 96-well plates for two weeks. To obtain a clone secreting a high level of Enpp1, we evaluated the clones by measuring the phosphodiesterase activity in culture supernatants using *p*NP-TMP as a substrate, as described by Hamdan *et al.* (2002). For large-scale expression, the selected stable cells were cultured at 310 K for three weeks in DMEM medium (Sigma) supplemented with 10%(*v*/*v*) FBS (Euro Clone), 1%(*v*/*v*) MEM non-essential amino acids (Sigma) and 1%(*v*/*v*) sodium pyruvate (Gibco) using a BelloCell bioreactor (CESCO Bioengineering) connected to a medium circulating system with a 2.5 l reservoir. To produce selenomethionine-labelled Enpp1, the stable cells were cultured in methionine-free medium (Gibco) supplemented with 50 mg l^{-1} L-selenomethionine (SeMet; Wako) and 63 mg l^{-1} L-cystine (Sigma).

2.3. Purification

The culture supernatant (1 l) was clarified by centrifugation followed by filtration using a 0.45 µm bottle-top filter (Millipore). The pH of the supernatant was adjusted to 7.5 with 1 *M* Tris–HCl pH 7.5. The supernatant was mixed with P20.1-Sepharose resin (10 ml) at 277 K overnight and the mixture was then loaded into an Econo-Column (1.5 × 15 cm; Bio-Rad). The resin was washed with 50 ml buffer *A* (20 m*M* Tris–HCl pH 7.5, 150 m*M* NaCl) and the protein was eluted with the same buffer containing 0.2 mg ml^{-1} PRGY-PGQV peptide. The eluted fraction (40 ml) was concentrated to 5 ml using a Vivaspin 20 filter (30 kDa molecular-weight cutoff; GE Healthcare) and then mixed with TEV protease [0.37 mg, 1:10(*w*:*w*)] at 293 K overnight to remove the TARGET tag. The protein was further purified on a HiLoad Superdex 200 16/60 gel-filtration column (GE Healthcare) equilibrated with buffer *B* (5 m*M* Tris–HCl pH 7.5, 150 m*M* NaCl). The purified protein was concentrated to 7 mg ml^{-1} using a Vivaspin 2 filter (30 kDa molecular-weight cutoff; GE Healthcare) and stored at 193 K until use. The purity of the protein was assessed by SDS–PAGE and the gels were stained with SimplyBlue SafeStain (Invitrogen).

2.4. Crystallization

Initial crystallization screening was performed at 293 K by the sitting-drop vapour-diffusion method in a 96-well Intelli-Plate (Hampton Research) using the following screening kits: Crystal Screen, Crystal Screen 2, PEG/Ion, Index, Natrix and SaltRX (Hampton Research), PACT and JCSG (Qiagen) and MemGold (Molecular Dimensions). Crystallization droplets were prepared by mixing 100 nl protein solution (5 mg ml^{-1} in 5 m*M* Tris–HCl pH 7.5, 150 m*M* NaCl, 0.2 m*M* zinc sulfate, 10 m*M* AMP) and 100 nl reservoir solution using a Mosquito crystallization robot (TTP LabTech). Initial hits were optimized at 293 K using the hanging-drop vapour-diffusion method by manually mixing 1 µl protein solution and 1 µl reservoir solution. Additive Screen (Hampton Research) was also used for optimization of the crystallization conditions.

2.5. Data collection and preliminary crystallographic analysis

Crystals were cryoprotected in reservoir solution supplemented with 30%(*v*/*v*) glycerol and were flash-cooled in a nitrogen-gas stream at 100 K. All X-ray diffraction experiments were performed on beamline BL32XU at SPring-8, Hyogo, Japan using an MX225HE detector. To reduce radiation damage, the crystals were mounted on a nylon loop (Hampton) with the longest dimension of the crystal oriented along the spindle axis and were successively translated along the longest dimension during data collection. A native data set was collected using a microbeam (8 × 11.6 µm) at a wavelength of 1 Å with an oscillation angle of 180° (1° per frame), an exposure time of 1 s per frame and an attenuator thickness of 400 µm; the crystal was gradually translated every six frames. A SAD data set was collected from an SeMet-labelled crystal using a microbeam (1 × 15 µm) at a wavelength of 0.9790 Å (the Se peak) with an oscillation angle of 360° (1° per frame) and an exposure time of 1 s per frame; the crystal was gradually translated after each frame. No attenuation was used. Data were processed using *HKL*-2000 (Otwinowski & Minor, 1997). Molecular replacement was performed in *MOLREP* (Vagin & Teplyakov, 2010), using the structure of mouse Enpp2 (PDB entry 3nkm; Nishimasu *et al.*, 2011) as the search model, to identify the Se sites. The anomalous difference Fourier map was calculated based on the SAD data set using *PHENIX* (Adams *et al.*, 2002). The experimental phase was determined using *SHARP* (de La Fortelle & Bricogne, 1997), followed by solvent flattening and noncrystallographic symmetry (NCS) averaging using *RESOLVE* (Terwilliger & Berendzen, 1999). Model building and refinement were performed using *Coot* (Emsley & Cowtan, 2004) and *PHENIX* (Adams *et al.*, 2002), respectively.

3. Results and discussion

3.1. Protein preparation

Enpp1 is a type II single-membrane-spanning protein and contains an N-terminal transmembrane region, whereas Enpp2 is a secreted

protein and contains an N-terminal secretory signal sequence. To obtain the extracellular region of Enpp1 as a soluble protein, we replaced the transmembrane region of mouse Enpp1 with the secretory signal sequence of mouse Enpp2 (Fig. 1*a*). Since nine putative N-glycosylation sites are present in the extracellular region, we expressed the engineered recombinant protein in *N*-acetylglucosaminyltransferase-deficient HEK293S cells, which produce homogeneously glycosylated proteins that are suitable for crystallization (Reeves *et al.*, 2002). Fusion of the secretory signal sequence increased the phosphodiesterase activity in the culture supernatant by about tenfold, indicating that the signal sequence facilitated the secretion of the recombinant protein into the culture supernatant. Although the recombinant protein in the culture supernatant was not clearly detected on the gel after SDS–PAGE owing to its low expression levels, we successfully purified the protein as a single band on the SDS–PAGE gel using P20.1-Sepharose affinity

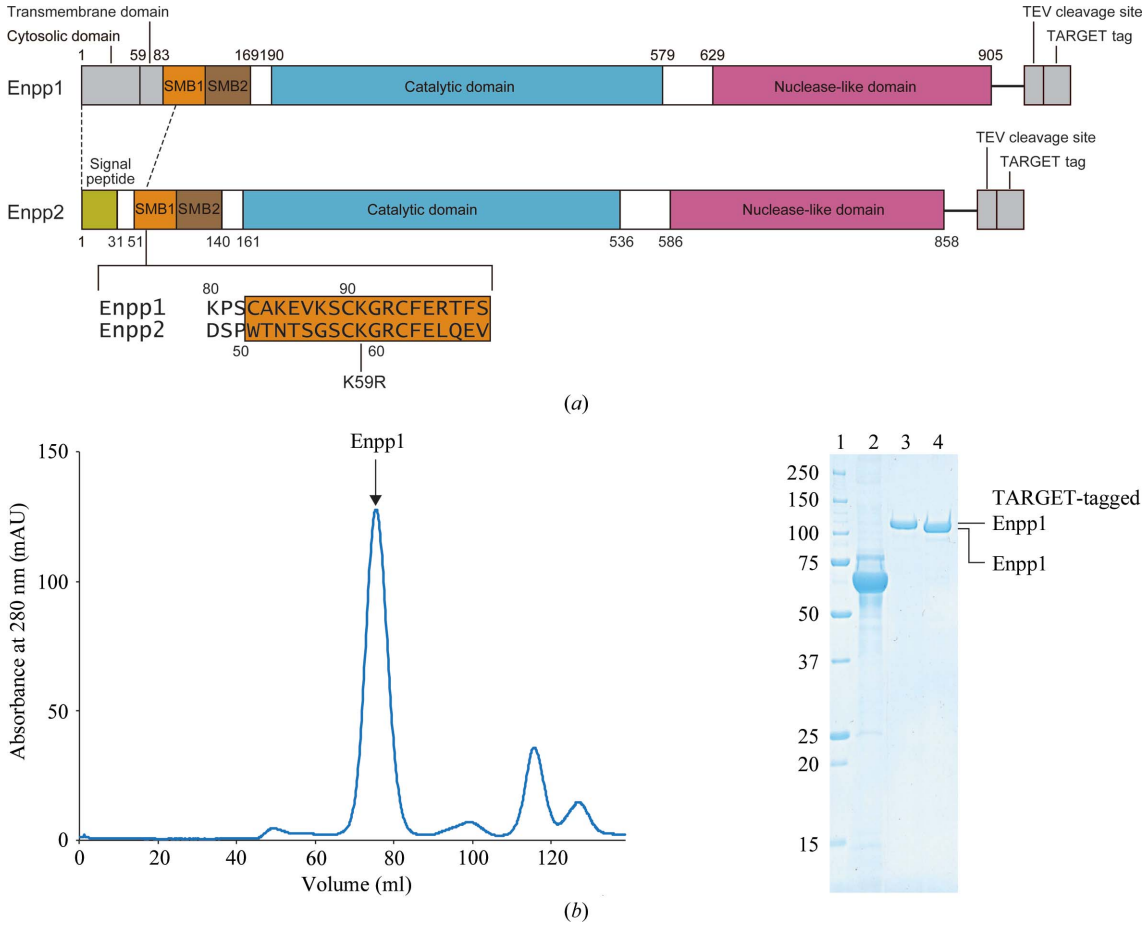

Figure 1
Preparation of the extracellular region of Enpp1. (*a*) Construction of Enpp1. The domain organizations of Enpp1 and Enpp2 and a sequence alignment of the N-terminal regions of their SMB1 domains are shown. (*b*) Purification of Enpp1. Proteins were analyzed by SDS–PAGE and stained with SimplyBlue SafeStain. Lane 1, molecular-weight markers (labelled in kDa); lane 2, culture supernatant; lane 3, C-terminally tagged Enpp1 protein after P20.1-Sepharose chromatography; lane 4, purified Enpp1 protein after cleavage of the TARGET tag and gel-filtration chromatography.

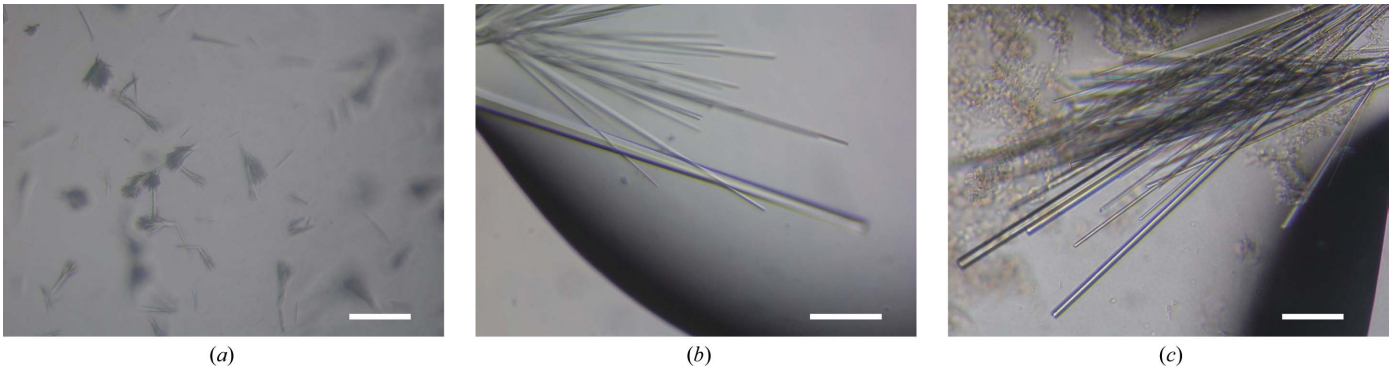

Figure 2
Crystals of Enpp1. (*a*) Native crystals obtained under the initial conditions. (*b*) Native crystals obtained under the refined conditions. (*c*) SeMet-labelled crystals obtained under the refined conditions. Scale bars indicate 100 µm.

Table 1
Data-collection statistics.

Values in parentheses are for the outer shell.

	Native	SeMet, peak
Beamline	BL32XU, SPring-8	BL32XU, SPring-8
Wavelength (Å)	1	0.979
Crystal-to-detector distance (mm)	264	300
Total oscillation range (°)	180	360
Oscillation range (°)	1	1
Exposure time (s)	1	1
Space group	$P3_1$	$P3_1$
Unit-cell parameters (Å)	$a = b = 104.4$, $c = 175.9$	$a = b = 105.3$, $c = 173.7$
Resolution (Å)	50–3.00 (3.05–3.00)	50–2.70 (2.75–2.70)
Total reflections	143009	446607
Unique reflections	41956	58639
Multiplicity	3.5 (2.3)	7.6 (4.7)
Completeness (%)	96.9 (91.0)	99.7 (97.5)
$\langle I/\sigma(I)\rangle$	11.8 (1.8)	8.0 (1.9)
$R_{\rm merge}$	0.157 (0.414)	0.206 (0.533)

chromatography (Fig. 1*b*). These results highlight the usefulness of the TARGET tag/P20.1-Sepharose system for purifying a trace amount of a target protein from a crude sample. The protein was further purified by gel-filtration chromatography and was eluted at a volume corresponding to a molecular weight of 85 kDa (Fig. 1*b*), which is close to the molecular weight deduced from its amino-acid sequence (94 kDa). These results indicated that the extracellular region of Enpp1 exists as a monomer. Finally, 1.4 mg purified protein was obtained from 1 l culture supernatant. We confirmed that it displayed phosphodiesterase activity (data not shown).

3.2. Crystallization

Initially, needle-shaped crystals were obtained using condition No. 38 of MemGold [28%(*v*/*v*) PEG 400, 50 m*M* sodium acetate pH 5.0, 50 m*M* magnesium acetate; Fig. 2*a*]. This initial condition was optimized by varying the pH, the types and concentrations of salt and the PEG in the reservoir solution. Optimization using Additive Screen revealed that larger crystals could be grown in the presence of polyvinyl propylene. Finally, thin rod-shaped crystals with dimensions of 30 × 30 × 500 µm were obtained under crystallization conditions consisting of 18%(*v*/*v*) PEG 600, 50 m*M* sodium acetate pH 4.5, 50 m*M* magnesium acetate, 0.5%(*w*/*v*) polyvinyl propylene (Fig. 2*b*). SeMet-labelled crystals were obtained under conditions similar to those used for the native protein (Fig. 2*c*). We also tried to crystallize Enpp1 expressed in Sf9 insect cells. However, the protein did not produce diffraction-quality crystals, although it was monodisperse on size-exclusion chromatography (data not shown). These results suggested that in contrast to the protein prepared from HEK293S GnT1$^-$ cells, the protein prepared from Sf9 cells had heterogeneous glycosylation modifications which may hamper crystallization by interfering with crystal packing.

3.3. Data collection and preliminary crystallographic analysis

To reduce radiation damage, all data sets were collected on the microfocus beamline BL32XU at SPring-8 using a helical data-collection strategy involving a microbeam. The native crystal diffracted to 3.0 Å resolution (Fig. 3*a*) and belonged to space group $P3_1$, with unit-cell parameters $a = b = 104.4$, $c = 175.9$ Å. The data-collection statistics are summarized in Table 1. Assuming the presence of two protein molecules per asymmetric unit, the Matthews coefficient ($V_{\rm M}$) was estimated to be 3.39 Å^3 Da^{-1}, with a solvent content of 64%. Molecular replacement was performed using the structure of mouse Enpp2 (PDB entry 3nkm; 44% sequence identity; Nishimasu *et al.*, 2011) as a search model, which provided a solution. After solvent flattening and NCS averaging, the resulting electron-density map showed a clear solvent–protein boundary. However, model building was not successful (the $R_{\rm free}$ value did not decrease below 35%); the electron-density map did not show distinctive

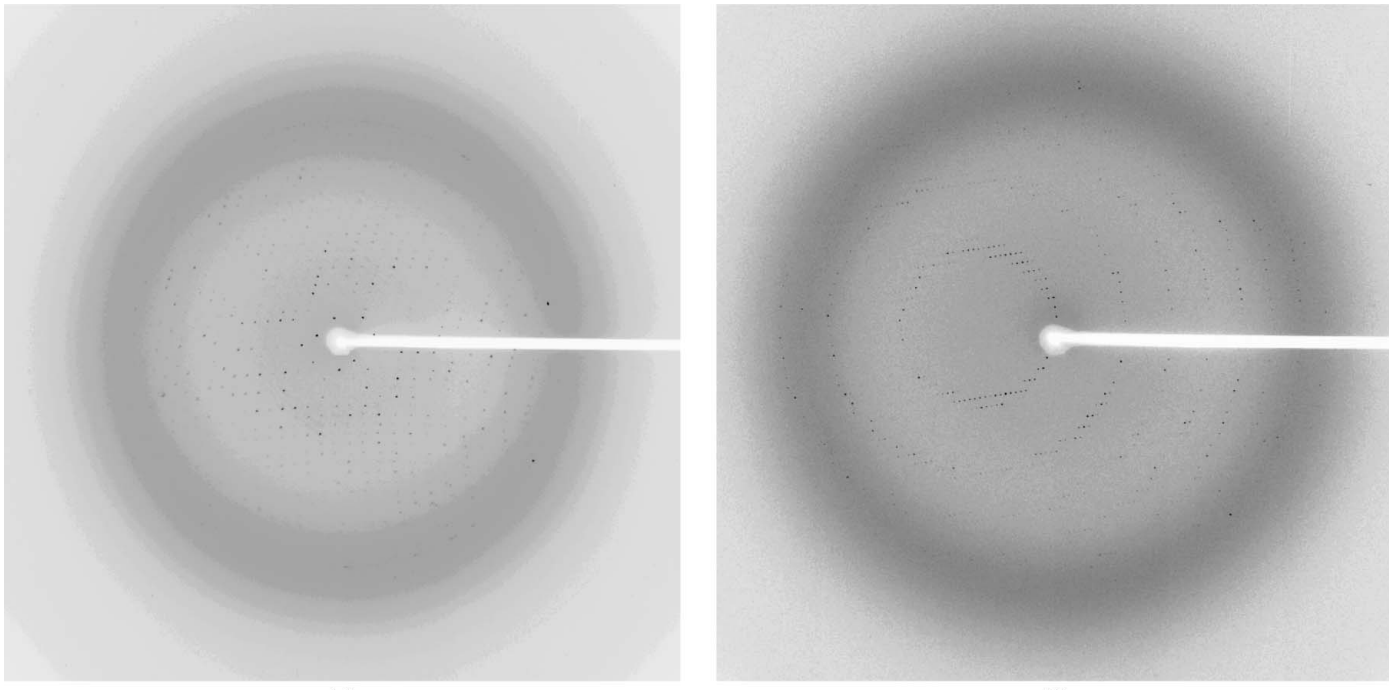

(*a*) (*b*)

Figure 3
X-ray diffraction patterns of Enpp1. (*a*) Diffraction pattern of the native crystal. (*b*) Diffraction pattern of the SeMet-labelled crystal.

features of the correct structure owing to model bias. The SeMet-labelled crystal diffracted to 2.7 Å resolution (Fig. 3*b*) and belonged to space group $P3_1$, with unit-cell parameters $a = b = 105.3$, $c = 173.7$ Å. An anomalous difference Fourier map calculated using the SAD data set and the phases derived from molecular replacement revealed 24 Se sites per asymmetric unit. The initial phase was determined using the Se sites and was followed by solvent flattening and NCS averaging, which resulted in an interpretable electron-density map. Model building and structural refinement are now in progress.

We thank the beamline staff at BL32XU at SPring-8 for technical help during data collection. This work was supported by grants to ON from the Japan Society for the Promotion of Science (JSPS) through its 'Funding Program for World-Leading Innovative R&D on Science and Technology (FIRST program)' and the Core Research for Evolutional Science and Technology (CREST) Program 'The Creation of Basic Medical Technologies to Clarify and Control the Mechanisms Underlying Chronic Inflammation' of Japan Science and Technology Agency (JST), by a Grant-in-Aid for Scientific Research on Innovative Areas from MEXT to RI and ON, and by Grants-in-Aid for Scientific Research (S) and (A) from MEXT to ON and HN, respectively.

References

Adams, P. D., Grosse-Kunstleve, R. W., Hung, L.-W., Ioerger, T. R., McCoy, A. J., Moriarty, N. W., Read, R. J., Sacchettini, J. C., Sauter, N. K. & Terwilliger, T. C. (2002). *Acta Cryst.* D**58**, 1948–1954.
Emsley, P. & Cowtan, K. (2004). *Acta Cryst.* D**60**, 2126–2132.
Hamdan, S., Bulloch, E. M., Thompson, P. R., Beck, J. L., Yang, J. Y., Crowther, J. A., Lilley, P. E., Carr, P. D., Ollis, D. L., Brown, S. E. & Dixon, N. E. (2002). *Biochemistry*, **41**, 5266–5275.
Hausmann, J. *et al.* (2011). *Nature Struct. Mol. Biol.* **18**, 198–204.
Hessle, L., Johnson, K. A., Anderson, H. C., Narisawa, S., Sali, A., Goding, J. W., Terkeltaub, R. & Millan, J. L. (2002). *Proc. Natl Acad. Sci. USA*, **99**, 9445–9449.
La Fortelle, E. de & Bricogne, G. (1997). *Methods Enzymol.* **276**, 472–494.
Nishimasu, H., Ishitani, R., Aoki, J. & Nureki, O. (2012). *Trends Pharmacol. Sci.* **33**, 138–145.
Nishimasu, H., Okudaira, S., Hama, K., Mihara, E., Dohmae, N., Inoue, A., Ishitani, R., Takagi, J., Aoki, J. & Nureki, O. (2011). *Nature Struct. Mol. Biol.* **18**, 205–212.
Otwinowski, Z. & Minor, W. (1997). *Methods Enzymol.* **276**, 307–326.
Reeves, P. J., Callewaert, N., Contreras, R. & Khorana, H. G. (2002). *Proc. Natl Acad. Sci. USA*, **99**, 13419–13424.
Rutsch, F. *et al.* (2003). *Nature Genet.* **34**, 379–381.
Stefan, C., Jansen, S. & Bollen, M. (2005). *Trends Biochem. Sci.* **30**, 542–550.
Tabata, S., Nampo, M., Mihara, E., Tamura-Kawakami, K., Fujii, I. & Takagi, J. (2010). *J. Proteomics*, **73**, 1777–1785.
Terwilliger, T. C. & Berendzen, J. (1999). *Acta Cryst.* D**55**, 849–861.
Vagin, A. & Teplyakov, A. (2010). *Acta Cryst.* D**66**, 22–25.